X-633-63-233

42 p.

N64 14280
CODE-1
(TMX-51388;

THE TRANSPORT PROPERTIES OF P-TYPE PbTe

OTS PRICE ✓

XEROX $ 4.60 ph.

MICROFILM $ 1.46 mf.

NOVEMBER 1963

(NASA

GODDARD SPACE FLIGHT CENTER

GREENBELT, MD.

602307

(over)

N64-14280

This material published by the Clearinghouse for Federal Scientific and Technical Information is for use by the public and may be reprinted except that where patent questions appear to be involved the usual preliminary search is advised, and where copyrighted material is used permission should be obtained for its further publication.

CLEARINGHOUSE

FOR FEDERAL SCIENTIFIC AND TECHNICAL INFORMATION

OF THE

U.S. DEPARTMENT OF COMMERCE

DOCUMENT TRANSMITTAL FORM

This transmittal form is intended to guide the NASA Scientific and Technical Information facility in processing scientific and technical reports and articles prepared under NASA contracts, subcontracts, and grants. It is also a processing guide for reports and articles produced by NASA activities when these publications do not appear in the regular NASA reports series (e.g., Technical Report, Technical Note, Technical Memorandum, Technical Translation, etc.).

The form is to accompany each unclassified and classified document transmitted for central indexing and reference or for processing and distribution. One copy of this form, accompanied by one or more copies of the document, should be sent to the following address:

Technical Information Division
Code 250
Greenbelt, Maryland

One of the types listed on the reverse side of this form (indicated by a numeral, and modified where necessary by alphabetical subheadings) should be selected for each document submitted. The following identifying information should also be furnished:

DOCUMENT TITLE: THE TRANSPORT PROPERTIES OF P-TYPE PbTe.		
ORIGINATING ORGANIZATION (DIVISION, BRANCH, SECTION): SPACECRAFT TECH. DIV.; THERMAL SYS BR.; RADIATION EFFECT SEC.		
REPORT NO.: X-633-63-233	DATE OF DOCUMENT: NOVEMBER 1963	NO. OF COPIES ENCLOSED: 2
SECURITY CLASSIFICATION OF DOCUMENT: NONE		
IF CLASSIFIED: TITLE CLASSIFICATION	ABSTRACT CLASSIFICATION: SOLID STATE PHYSICS	
CONTRACT, SUBCONTRACT, OR GRANT NO.: NONE		
GSFC OFFICE TRANSMITTING DOCUMENT: BY: Martin M. Skolnik 633 Spacecraft Engineer (SIGNATURE AND TITLE)		
DATE TRANSMITTED: Dec 20, 1963	DOCUMENT TYPE: (APPROPRIATE NUMERAL AND LETTER SELECTED FROM BACK) 7D	

GSFC 25-13 (11-62)

DOCUMENT TYPES

1. ☐ Report is unclassified and is suitable for unlimited announcement and distribution to the aeronautics and space community, and for public sale.

2. ☐ Report is unclassified, but contains information of limited usefulness and does not justify widespread automatic distribution to the aeronautical and space community. It can, however, be announced and made publicly available.

3. ☐ Report is unclassified, but for official reasons, must be restricted as follows:

   a. ☐ Government agencies and their contractors only.
   b. ☐ Government agencies only.
   c. ☐ NASA activities only.

4. ☐ Report bears a security classification and is suitable for distribution within the limits of security considerations to:

   a. ☐ Government agencies and their contractors only.
   b. ☐ Government agencies only.
   c. ☐ NASA activities only.

5. ☐ Reprint of a journal article reporting NASA-supported work.

6. ☐ Article prepared for journal publication (preprint or other copy) reporting NASA-supported work. (Normally handled as No. 2 above.)

   Estimated date of publication: _____

7. ☒ Material for presentation at a meeting or conference.

   Name of Meeting: _____ Date: _____

   Sponsor(s): _____

   a. ☐ Scheduled for publication in proceedings. (Normally handled as No. 2 above.)

      Estimated date of publication: _____

   Not scheduled for publication in proceedings and subject to the following limitations or announcement and dissemination:

   b. ☐ Government agencies and their contractors only.
   c. ☐ Government agencies only.
   d. ☒ NASA Activities only.

THE TRANSPORT PROPERTIES OF P-TYPE PbTe

By

Martin M. Sokoloski
Goddard Space Flight Center

and

John H. Marburger III*
Stanford University
Palo Alto, Calif.

(Stanford U.) Nov. 1963
42 p refs

a contract

1 Code only

TABLE OF CONTENTS

INTRODUCTION

I. Motivation

Although lead telluride is now widely used in thermoelectric devices, there exists considerable confusion about the precise mechanisms responsible for its characteristic properties. In particular, no clear mechanism has been proposed which accounts for the $T^{-5/2}$ temperature dependence of the mobility. This law is obeyed for both holes and electrons over a very wide temperature range.

The difficulty of devising any theoretical model for PbTe can be appreciated by considering the numerous effects which must be explained.

Nearly all of these effects have been studied previously in connection with PbTe as well as with other semiconductors. Until now, however, no one has measured all the effects in a single sample and attempted to take them all into consideration in a single data reduction program. Such a procedure would be illuminating at the very least.

There is some evidence that the unusual temperature dependence of the mobility in PbTe can be accounted for by a temperature dependent effective mass. However there has been no attempt to apply this hypothesis at high temperatures. Furthermore at low temperatures the effects of degenerate electron statistics have never been considered in detail although it is possible to do so. Thus, by painstaking use of present theoretical concepts and careful comparison with data obtained from samples of PbTe under a wide range of conditions, it may be possible to clarify the mechanisms operative in this material. The approach is thus not to search for new properties of PbTe, but rather to discover whether the known properties are consistent with a single synthesis of theoretical mechanisms.

II. Procedure

Nearly all the elementary parameters which appear in the theoretical expressions for mobility can be determined from measurements

of transport properties. In particular measurements of the Hall coefficient give information on the number of charge carriers, the one parameter most likely to change from sample to sample. Measurements of the conductivity and thermoelectric power give information about the mobility and Fermi level respectively. These measurements may be supplemented with other data in the literature to provide the basis for quantitative theorectical predictions. Part I of this paper discusses in detail how these predictions are to be made.

III. Present Stage of Progress

At this time, extensive measurements have been made on a sample of P-type PbTe. The apparatus and measuring techniques employed have been described in a previous report. Section II of this paper describes some modifications of the instrumentation and Section IV the accuracy of results obtained with it.

All results to date are in excellent agreement with those of other workers.

EXPERIMENTAL

SECTION I

DISCUSSION OF PbTe

Lead telluride is a IV-VI compound semiconductor having a crystal structure of the NaCl type. The bonding in a material of this type is expected to be strongly ionic, and the dominant scattering mechanism to be optical mode lattice scattering. However, this type of scattering does not lead to the observed temperature dependence of the mobility.

No explanation has yet been advanced for the failure of optical mode scattering to yield correct results for PbTe, but a recent attempt to synthesize the observed variation from a combination of acoustical and optical mode scattering seems promising (Reference 1). Nevertheless, such attempts are seriously complicated because before any information concerning the temperature dependence of the mobilities can be inferred from experiment, an evaluation of the temperature dependence of all quantities in the expressions relating the mobility to the observables must be initiated. Knowledge of the effective masses and anisotropies at all temperatures is essential. The following account of the structure of PbTe has been pieced together from past and present measurements of the transport effects including some made in very strong magnetic fields at 4.2°K.

The structure of the conduction band in PbTe is of the "many valley" type, i.e., it consists of several anisotropic minima distributed in k-space to satisfy the symmetry of the crystal. The constant energy surfaces are prolate spheroids whose major axes lie in the <111> direction in crystal momentum space. Since the minima occur at the edge of the Brillouin zone, there are only four ellipsoids. The ratio of major to minor axis is on the order of 5, but there is evidence that it decreases with temperature. The average effective mass (density of states) varies with temperature from about 0.14 at 77°K to 0.25 at 300°K. (Reference 2).

The valence band has two distinct sets of minima. The first set dominating the transport properties at low temperatures is similar in structure to the conduction band except for the effective mass values. It is difficult of measure the anisotropy of the spheroids in the first set,

since a second spherical set of surfaces located at k = 0 also contains holes at low temperatures and contributes to the conduction process. An average effective mass may be defined by reducing the data as if only one band were present. This effective mass apparently increases with temperature (Reference 1). A third set of surfaces, 0.1 ev from the first principal set, has been suggested (Reference 3). Section III gives a strong argument for the non-existence of such a third set of surfaces. The energy gap in PbTe is about 0.3 ev at $0^{\circ}K$ and increases with temperature at a rate of 4×10^{-4} ev/$^{\circ}K$. (Reference 4).

Measurements of the Hall mobility in p-type PbTe have shown a $T^{-5/2}$ dependence above about $200^{\circ}K$ and a (References 1, 3) $T^{-3/2}$ dependence below this temperature. Unfortunately in the latter range the hole statistics are no longer non-degenerate. No account has been taken of this to determine the temperature dependence of the actual mobility, but the maximum predicted effect of changing statistics has already been shown to be less than 15%. Another more serious difficulty of acoustical and optical mode lattice scattering mechanisms mentioned above indicates that the dominant scattering mechanism is changing at this temperature. This compounding of effects makes data reduction in this region a very difficult task.

All the effects mentioned above have been examined closely only at temperatures for which the material is extrinsic. Although measurements have been made in the intrinsic region, no attempt has been made to infer fundamental parameters from the data. Thus there is no real check on the mobility or effective mass temperature dependence at high temperatures. By detailed measurement of high field effects, these parameters may be inferred.

A further property of PbTe adds to the difficulty of examining this material: at high temperatures the material is unstable and the tellurium phase tends to precipitate out, changing the properties, impurity concentration, of the material considerably. Great caution must be exercised when making high temperature measurements on this material, otherwise the results may not be reproducible.

SECTION II

EXPERIMENTAL METHODS

A. APPARATUS AND METHOD OF DETERMINING THE HOMOGENEITY OF THE SAMPLE.

The existence of any large impurity gradients, p-n junctions, or other imperfections caused by sintering and doping the ingot can greatly affect the transport properties of the sample. As a result, before any measurements are to be made the percent deviation of the composition of the sample and the location of any p-n junctions must be determined.

A simplified version of the apparatus used by Cowles and Dauncey (Reference 5) for rapid scanning of the Seebeck coefficient of semiconductors was used.

From

$$\theta = -\frac{k}{e}\left\{2 - \frac{\epsilon^*}{kT}\right\}$$

and

$$n = \frac{2(2\pi m^* kT)^{\frac{3}{2}}}{h^3} \exp.\ \eta^*$$

where ϵ^* is the Fermi energy and $\eta = \epsilon/kT$ for a one band model with spherical energy surfaces obeying Boltzmann statistics. It is seen that the thermoelectric power, θ, is a sensitive function of the carrier concentration. Thus measuring the change of the Seebeck coefficient (thermoelectric power) along the sample at a constant temperature can yield the change of carrier concentration, including the existence of any p-n junctions.

Figure 2-1 shows the device actually used. With the switch on position #1, the direct temperature difference across the sample was recorded, while in position #2, the thermal electric voltage with respect to Chromel was recorded (absolute Seebeck voltages are not needed). The probe, whose tip was nickel plated to prevent the diffusion of copper into the sample, and the heater were connected to a micrometer slide, and the thermoelectric voltage versus distance along the specimen was noted. The results are given in Section III.

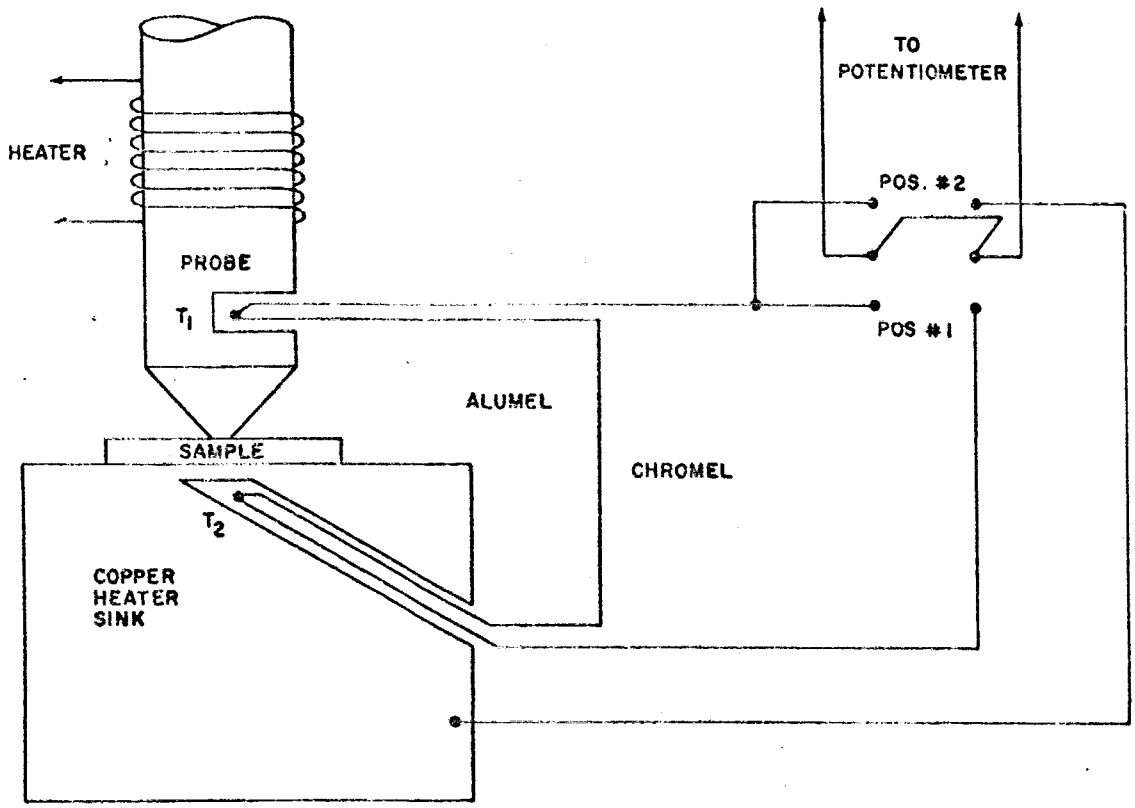

Figure 2-1—Schematic Wiring Diagram and Drawing of Homogeneity Apparatus After Cowles and Dauncy, Reference 1.

B. APPARATUS FOR MEASURING THE HALL COEFFICIENT, ELECTRICAL CONDUCTIVITY AND TRANSVERSE MAGNETO-RESISTIVITY.

The apparatus used to investigate the change of the Hall coefficient and electrical conductivity as a function of temperature, and of the Hall coefficient and magnetoresistivity as a function of magnetic field strength at various fixed temperatures is the same as that described in Reference 6, except for the following modifications. All leads coming out of the lid assembly shown in Figure 2 of Reference 6 were connected to box mounted receptacles which in turn were installed in a miniature chassis bolted on the top of the lid. To insure good electrical contact the pins and contacts of these receptacles were gold plated. This allowed all leads to be detached whenever the sample holder and lid assembly had to be taken out of the Hall cryostat.

The molybdenium pressure current contact springs shown in Figure 3 of Reference 6 were discarded and three platinum wires (0.002 inches in diameter) were attached approximately equidistantly

apart to each end of the sample by the capacitor discharge method. The use of three wires led to a more uniform electric field through the sample. Any probes which showed any non-ohmic characteristics were replaced.

The sample was etched with a solution of:

10 parts of saturated KOH solution
10 parts ethylene glycol
1 part of 3% hydrogen peroxide Reference 1.

The modified Wheatstone bridge circuit also described in Reference 6 was abandoned in favor of the DC method which proved to be more accurate. Figure 2-2 is a complete wiring diagram of the circuit. The Hall voltage recorded is not one half of the Hall voltage as stated in Reference 6 but is the total Hall voltage. A modified Schmidt trigger circuit was used to regulate the furnace. An error voltage (the difference between the output of a potentiometer and the true thermocouple voltage) was amplified and fed into the Schmidt trigger which fired the furnace when the error voltage exceeded a certain nominal value determined by the values of the components of the trigger. An automatic recorder was used to check the performance of the upper and lower sample thermocouples. The furnace regulating circuit kept the sample to within $\pm$ 2 degrees of the reading dialed on the potentiometer. Consequently, it was possible to determine Hall coefficient and magnetoresistivity values as a function of magnetic field strength at various fixed temperatures.

C. APPARATUS FOR MEASURING THE THERMOELECTRIC POWER AND NERNST COEFFICIENT.

The thermoelectric power in conjunction with the Hall coefficient can be used to determine the density of states effective mass, and with the thermal and electrical conductivities to determine the figure of merit, and finally to determine the position of the Fermi level.

Figure 2-3 shows various methods of measuring the thermoelectric power of semiconductors. There exist inherent difficulties in each of these configurations. For example: Method A provides poor thermal contact between the copper heater blocks and the sample, at the expense of recording the correct temperature gradient; while Method B gives inexact readings of the temperature gradient at the expense of good thermal contact. Since the thermoelectric power is a function of the temperature difference of the sample, any error in this measurement shows up in the thermoelectric power.

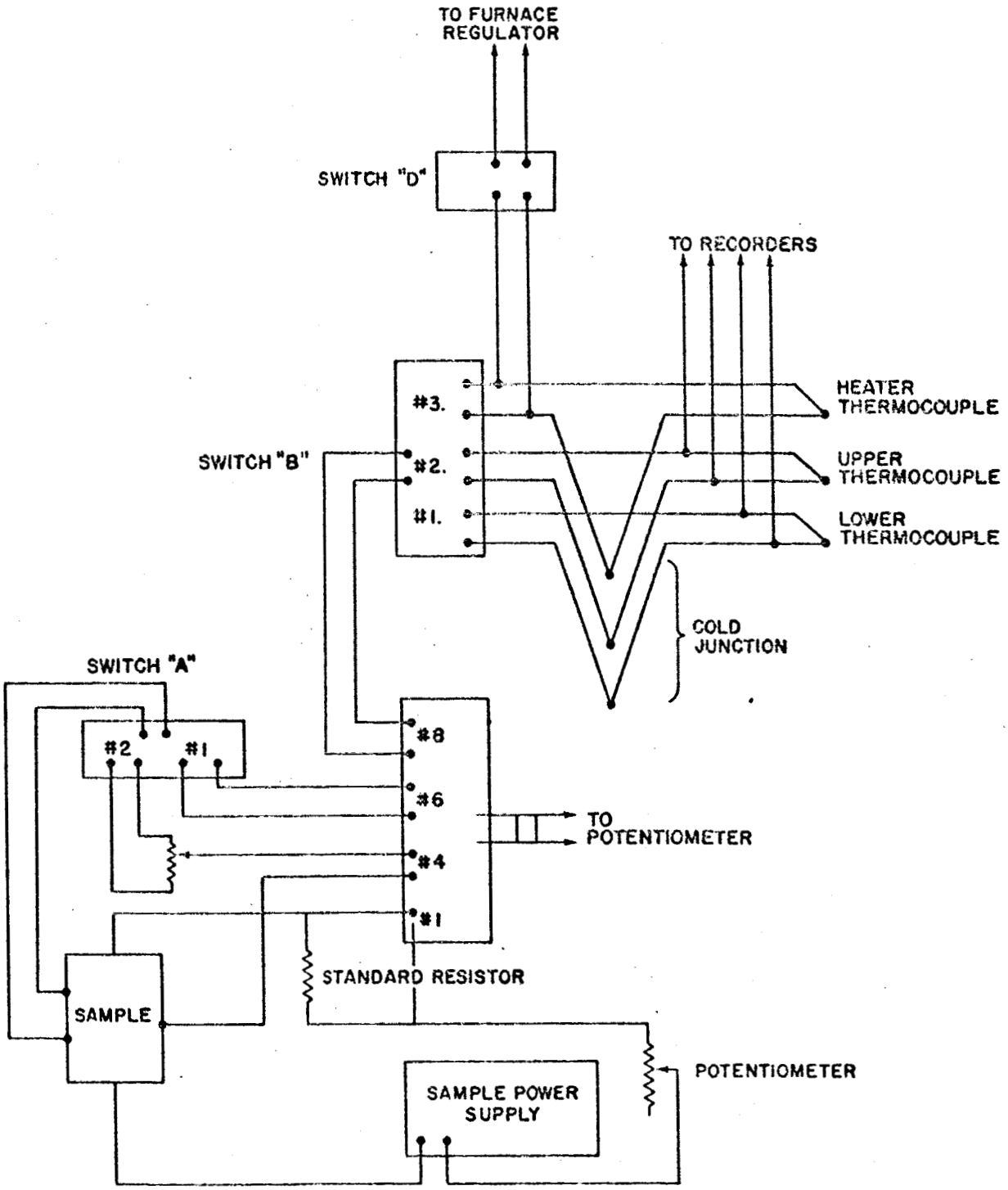

Figure 2-2—Schematic Wiring Diagram For Hall and Electrical Conductivity Experiment.

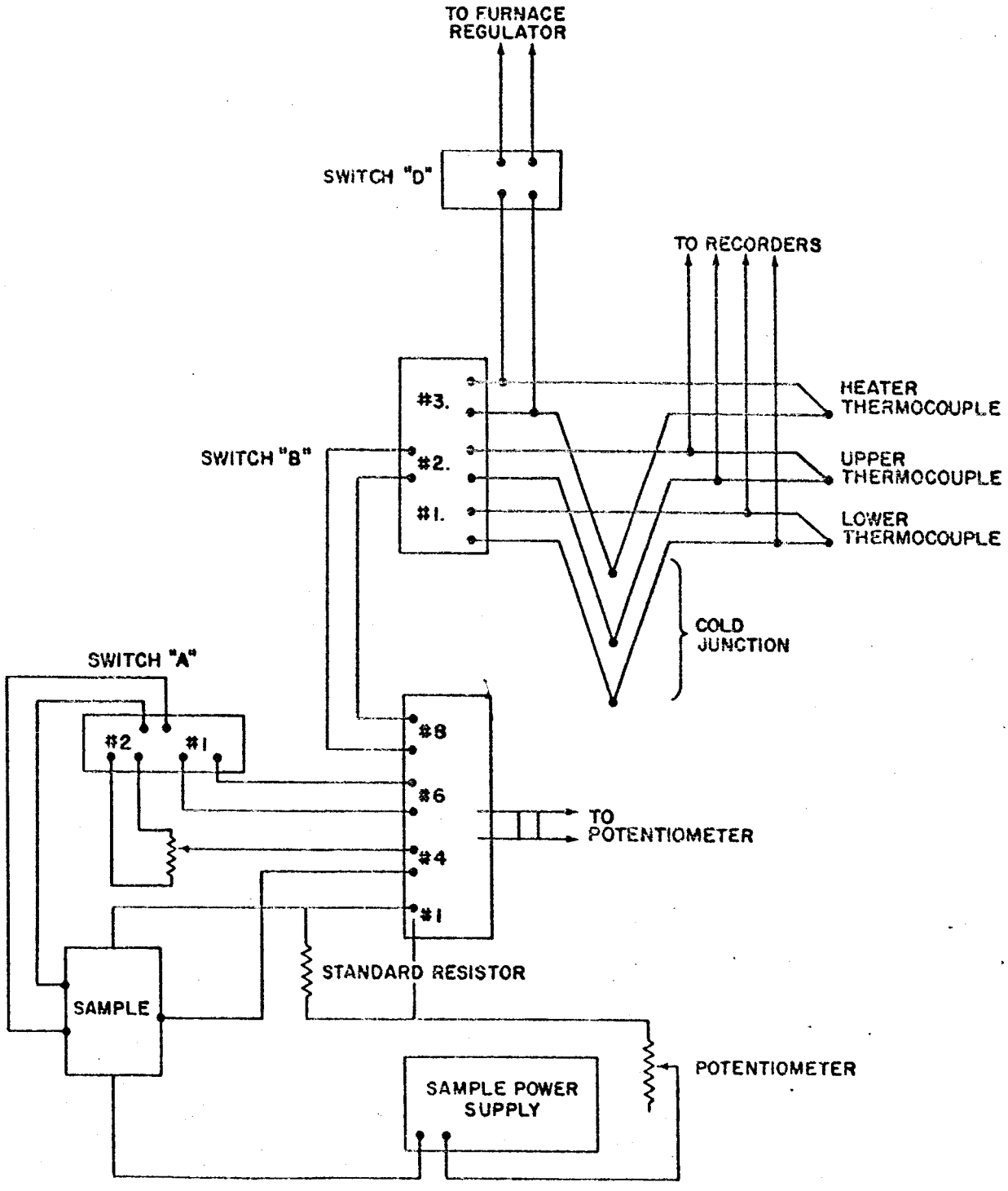

Figure 2-2—Schematic Wiring Diagram For Hall and Electrical Conductivity Experiment.

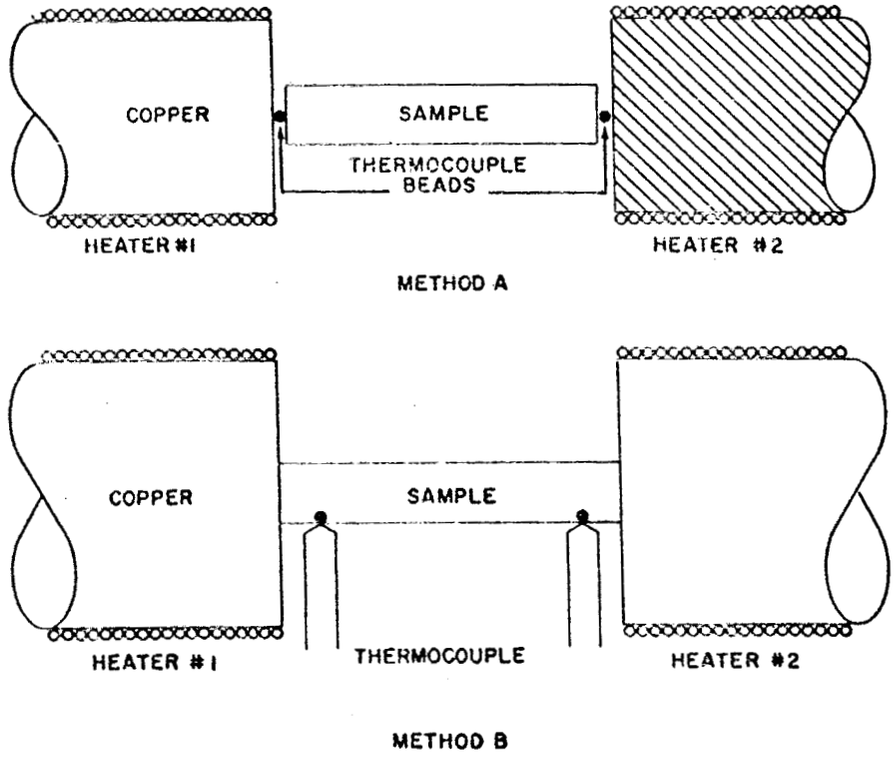

Figure 2-3—Schematic Arrangement for Various Methods of Measuring the Seebeck Voltage.

Figure 2-4 shows a design after Ioffe which minimizes the errors in configurations A and B (Reference 7). Since the ends of the sample are enclosed essentially in black body cavities, the thermocouples, if placed in the cavities, will record the correct temperatures while not affecting the thermal contact between the sample and the heater. In this arrangement, the thermocouples were attached to the ends of the sample and one leg of the thermocouples was used to measure the voltage difference. Because of this arrangement the absolute thermoelectric power of the material was not measured. Preliminary measurements using this apparatus were made on Bismuth Telluride and are mentioned in Section III.

A second thermoelectric power device shown in Figure 2-5 was designed to cover the range from liquid nitrogen temperatures to room temperatures and above. Some of the advantages of the former design have been retained.

Both designs can be used to measure the Nernst coefficient. All that needs to be added to the sample is a Hall probe type configuration and a magnetic field must be introduced perpendicular to the length of the sample.

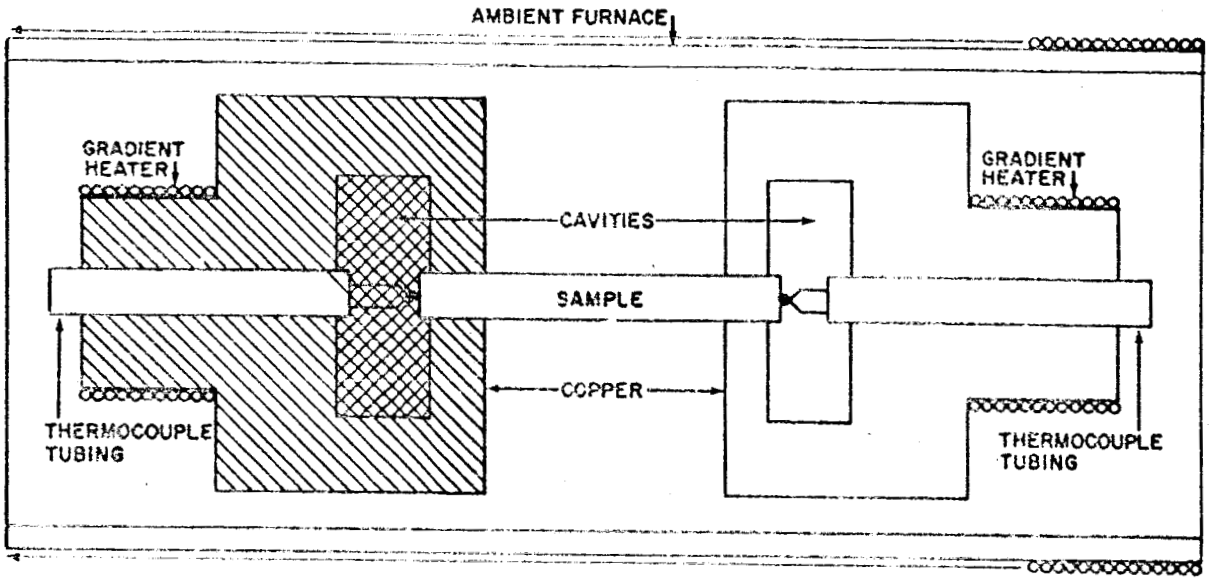

Figure 2-4—Configuration For The Elimination Of Temperature Errors In The Seebeck Apparatus After IOFFE.

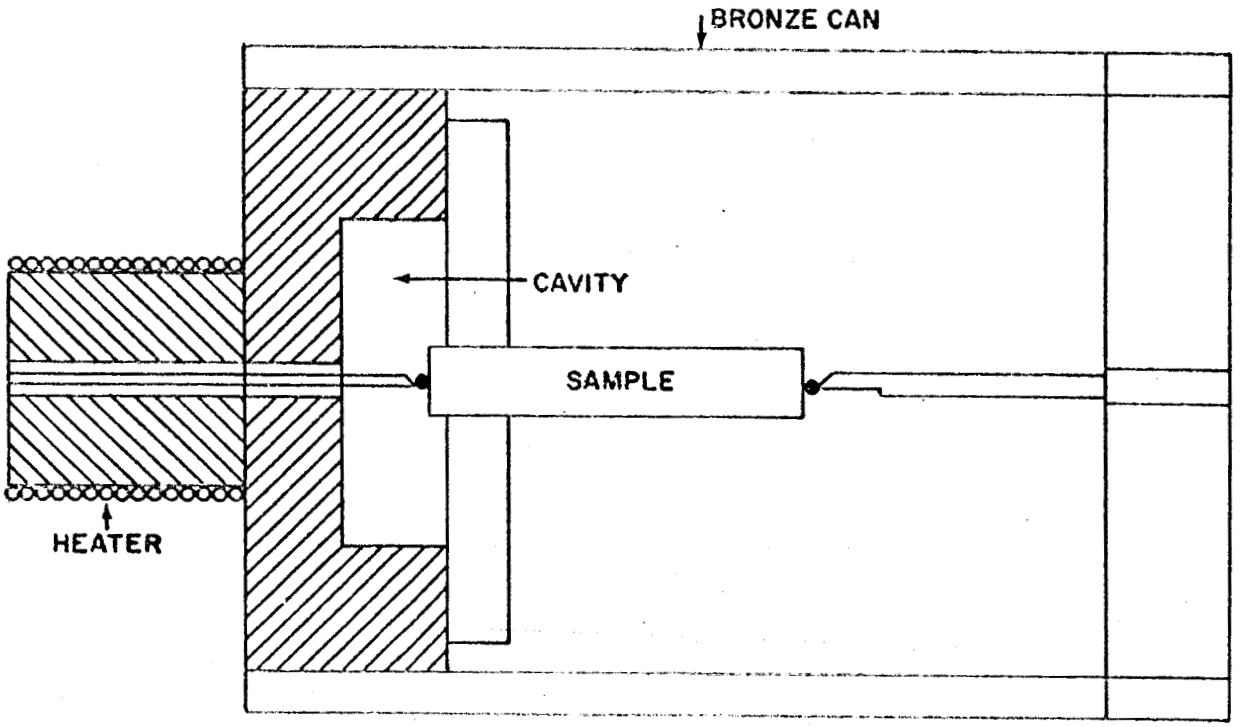

Figure 2-5—Modified Seebeck Apparatus For Below Room Temperature Measurements.

SECTION III

RESULTS

A. HOMOGENEITY EXPERIMENT

The homogeneity experiment was made on a p-type lead telluride polycrystalline ingot, doped with 10^{18} Cu atoms/cm^3. Reference 8 justifies extending most of the single crystal transport parameters (i.e., Hall coefficient, mobility, scattering, etc.) to polycrystalline samples in the temperature range from 79° to 594°K. The only objection would be the scattering of charge carriers by dislocations and grain boundaries, but this phenomena is prevalent only at extremely low temperatures (Reference 9). First, two flat faces were ground parallel on the cylindrical ingot, and a homogeneity test revealed a 4.1% carrier concentration deviation and no p-n junctions. It follows that any smaller section of the ingot should not have a carrier concentration deviation greater than 4.1%. Next, a rectangular Hall sample was cut from the ingot, and a homogeneity test revealed a 2.7% deviation and again no p-n junctions. This sample was used in the subsequent experiments.

B. THE HALL AND ELECTRICAL CONDUCTIVITY EXPERIMENT

Hall coefficients versus magnetic field strength curves are shown in Figures 2-6 and 2-7 for temperatures of 79°K and 293°K respectively. These figures demonstrate that the Hall coefficient is magnetic field independent for $\mu_H H/c < 1.26$ for the carrier concentration of 10^{18}. The Hall coefficient versus temperature runs were all made with a field strength of 3 kilogauss; therefore, the weak field approximation to the Hall coefficient can be used.

$$R = \frac{b}{n_o e}\left[\frac{3K(K+2)}{(2K+1)^2}\right] \qquad (2\text{-}1)$$

Here n_o is the total carrier concentration, e is the electronic charge, b is statistically dependent, and K is the ratio of the longitudinal to the transverse effective mass. From 79°K to 293°K a double run (twice up and twice down) was made, and these results are quite consistent and

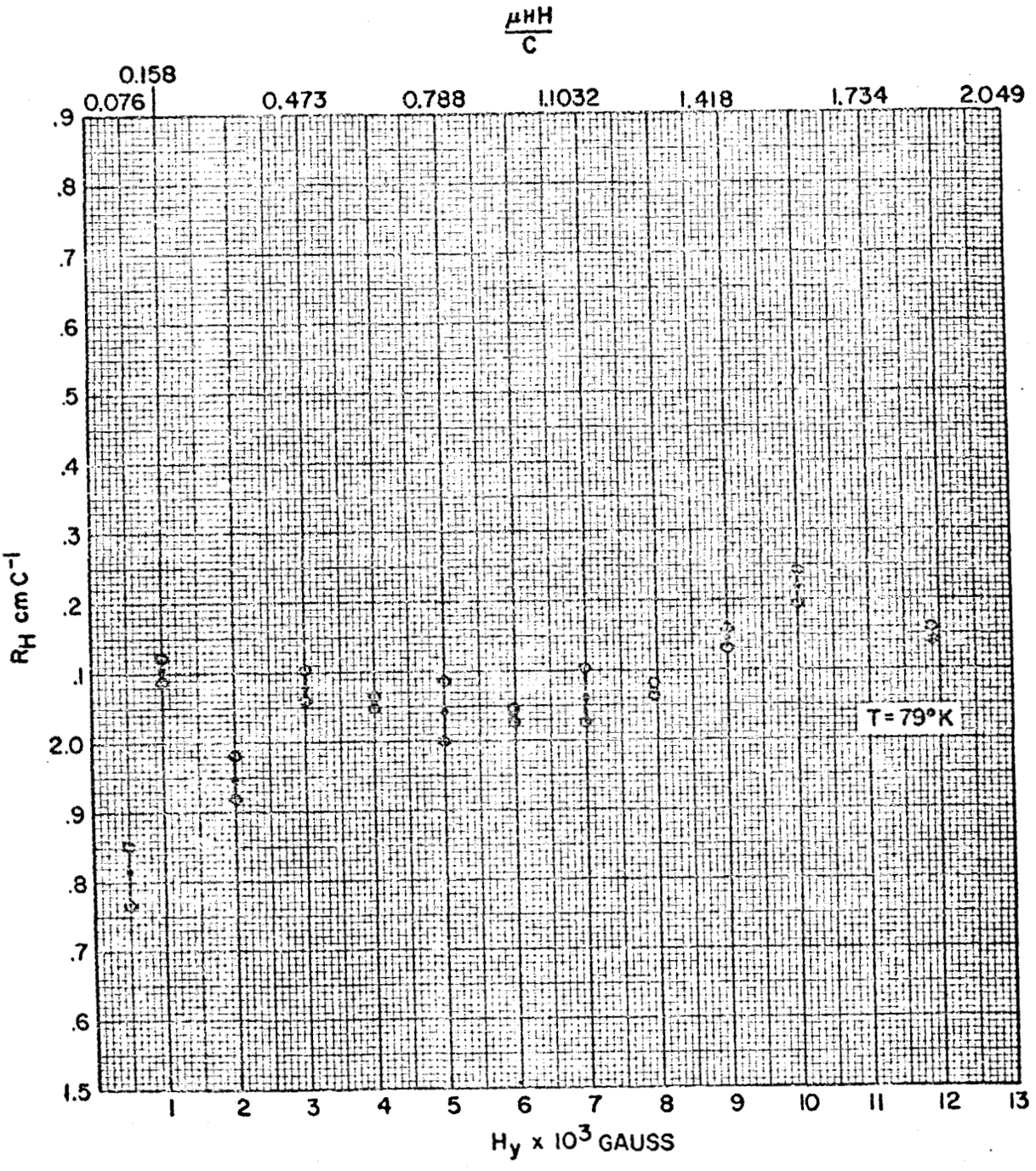

Figure 2-6—Hall Coefficient Versus Magnetic Field Strength At Liquid Nitrogen Temperature.

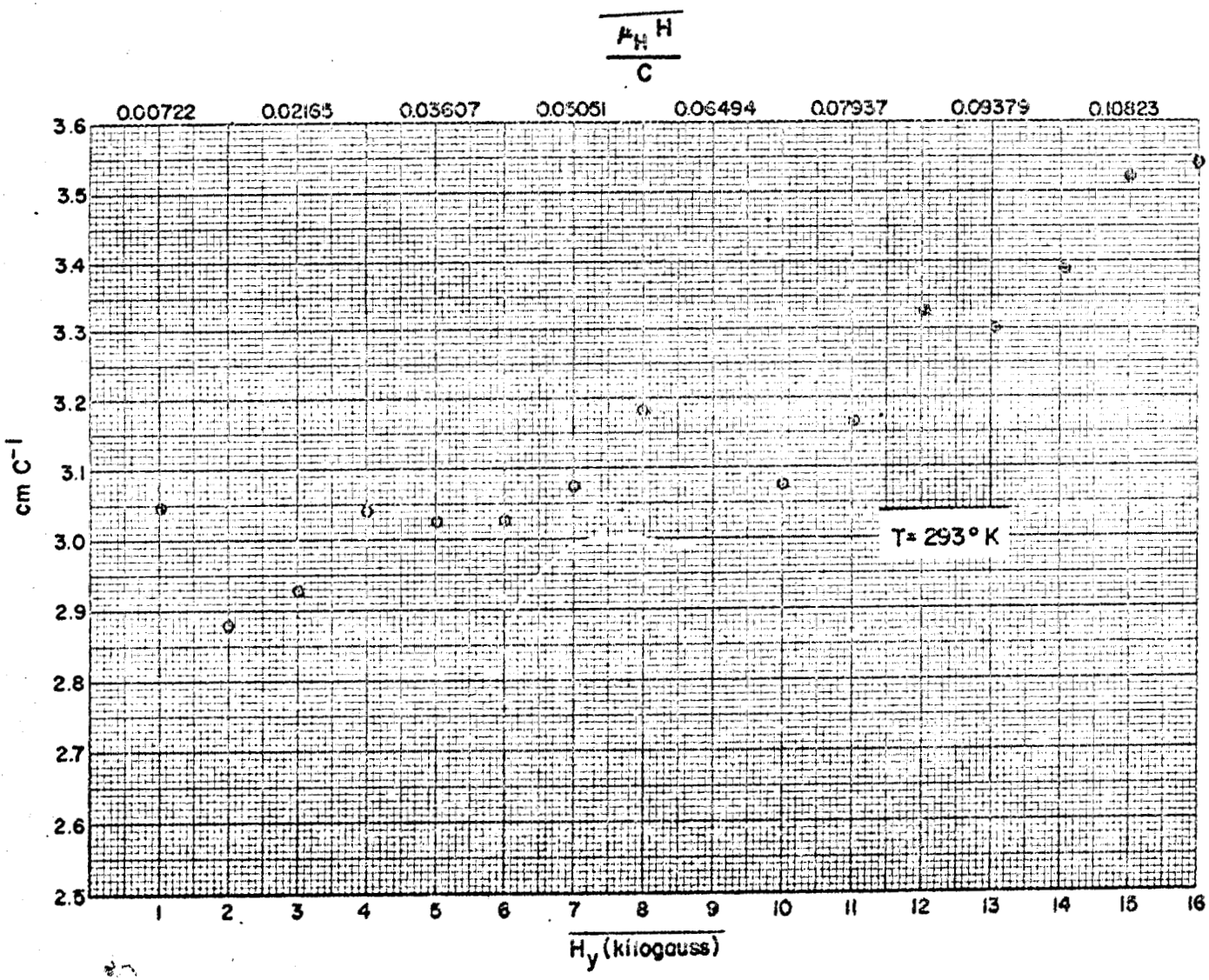

Figure 2-7—Hall Coefficient Versus Magnetic Field Strength At Room Temperature

reproducible. In Figure 2-8, the quantity $f(K) = 3K(K+2)/(2K+1)^2$ is plotted as a function of K to show the total variation of f(K) over the entire range of K. Mathematically, the most f(K) can change is by a factor of 25%, while for $3 < K < 5$, which is observed for p-type PbTe, the change in f(K) is at most 6%. At the same time the variation in b due to changing statistics is at most 15%. Therefore, the total theoretically observable change in the Hall coefficient in the extrinsic range should be no more than 20%. Nevertheless, a change greater than 40% is observed as can be seen in Figure 2-9. Figure 2-10 is a plot of Ln μ versus Ln T to show that at approximately $T = 150^{\circ}K$ the mobility is proportional to $T^{-5/2}$. The Hall coefficient is given by equation (2-1).

$$R_{79^{\circ}K} = \frac{b}{n_o e} f(K)$$

The conductivity for a two band carrier model is also given by,

$$\sigma(T) = n_1 e \mu_1(T) + n_2 e \mu_2(T) \qquad (2\text{-}2)$$

where n_1, $\mu_1(T)$ and n_2, $\mu_2(T)$ are the number of carriers and the mobilities in bands one and two respectively. Combining equations (2-1) and (2-2), results in,

$$R_{79^{\circ}K}\, \sigma(T) = bf(K) \left[AN_1 + BN_2\right] T^{-5/2} \quad \text{(Reference 3)} \qquad (2\text{-}3)$$

where N_1 and N_2 are the fractional amount of carriers in bands one and two respectively, (A and B are quantities which depend on the conductivity effective masses). Therefore, (Reference 10) a plot of $R_{79^{\circ}K}\, \sigma(T) \times (T/296^{\circ}K)^{5/2}$ versus 1/T should yield a straight line above $150^{\circ}K$, if conduction is due to only one band. This is indeed the case for n-type PbTe; however, from Figure 2-11, a "droop" similar to Allgaier's occurs above $150^{\circ}K$. This would support the argument for a second valence band assuming there is a transfer of carriers from n_1 to n_2. A plot of $Ln(R - R)/R_o$ versus 1/T as shown in Figure 2-12 should reveal an energy gap between these two valence bands (Reference 3). As can be seen the

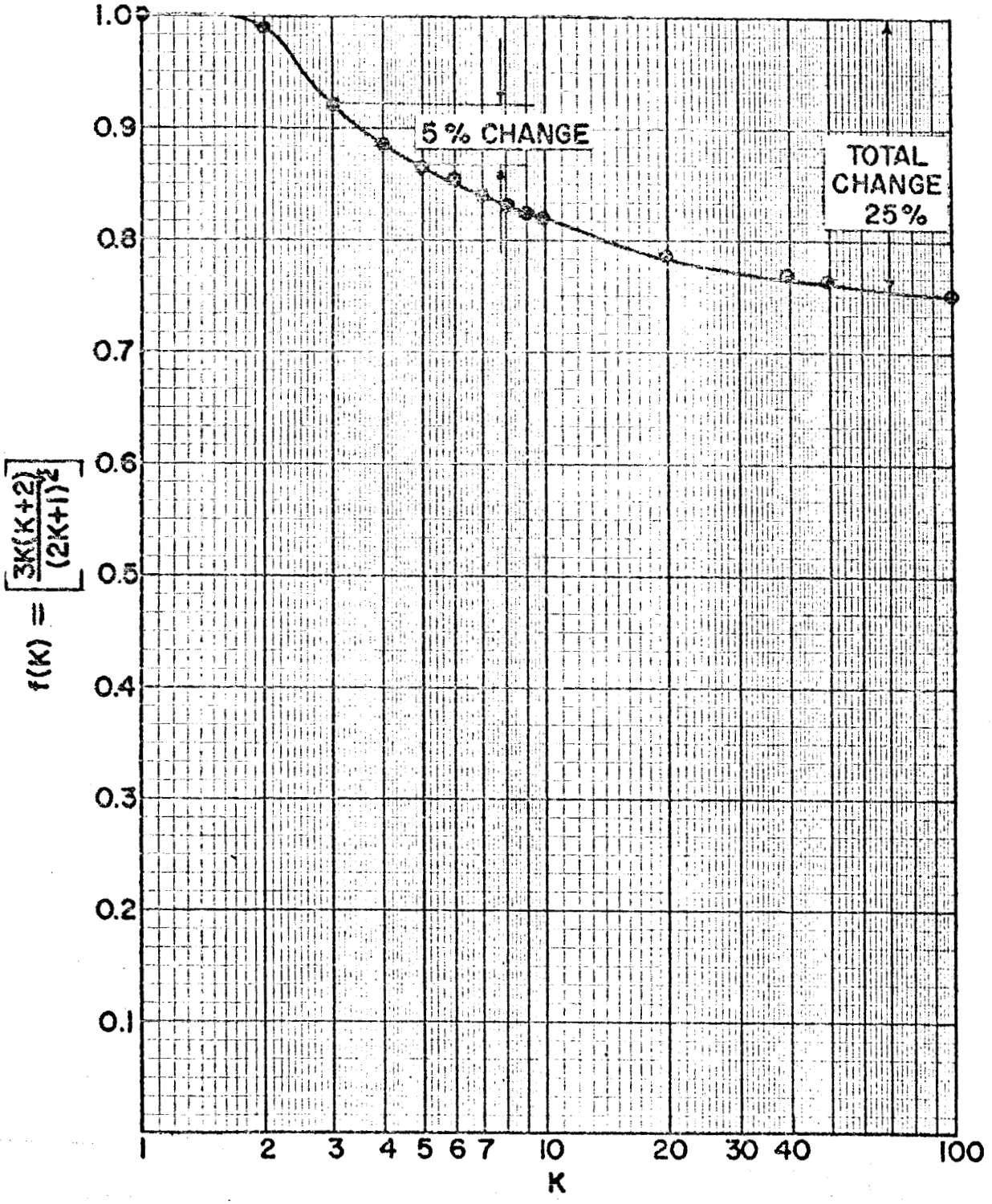

Figure 2-8--The Variation Of The Function $3K(K+2) / 2(K+1)^2$ Versus K For PbTe $3 < K < 5$.

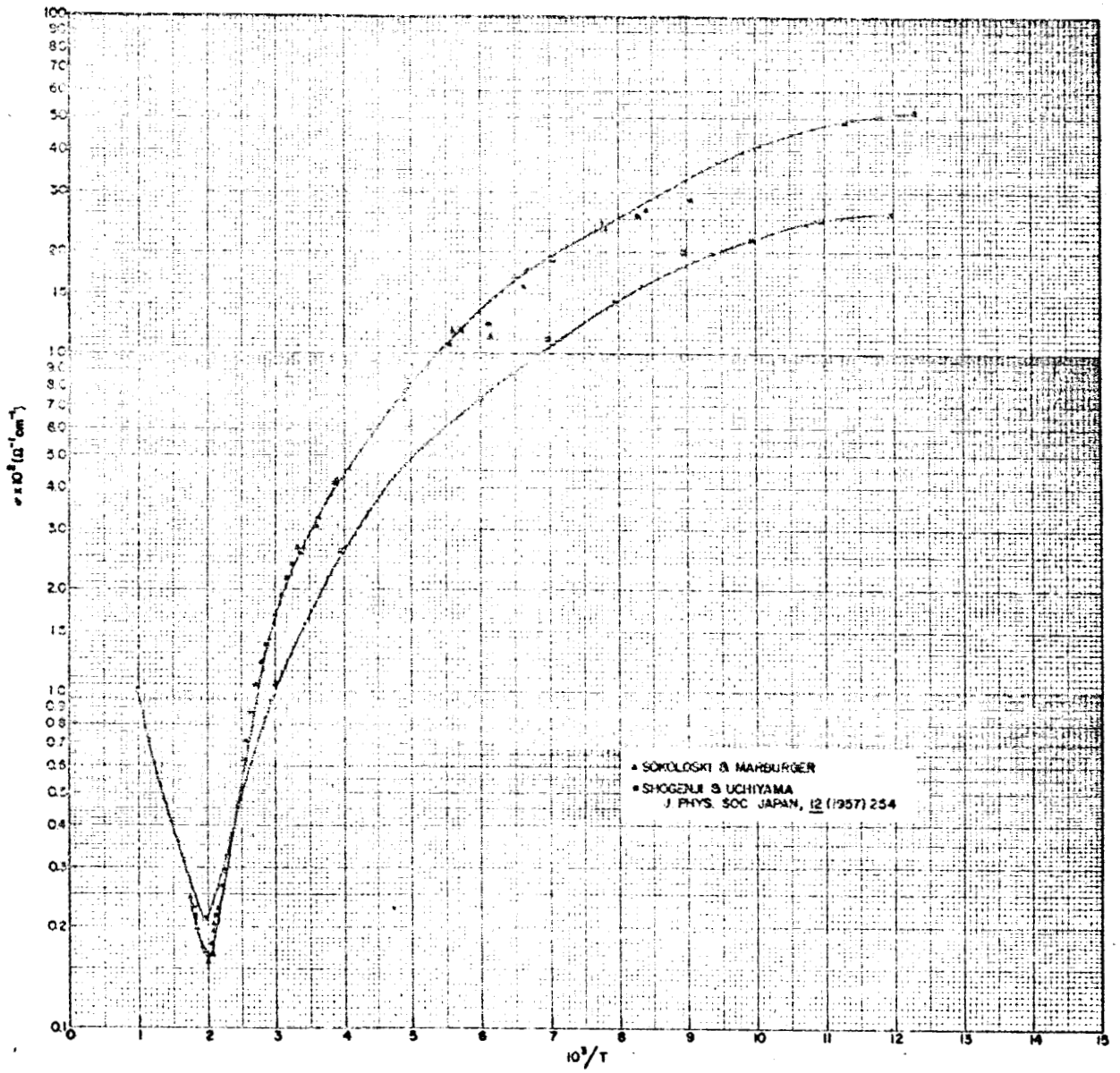

Figure 2-9—Log R_H Versus 1/T For p-type PbTe.

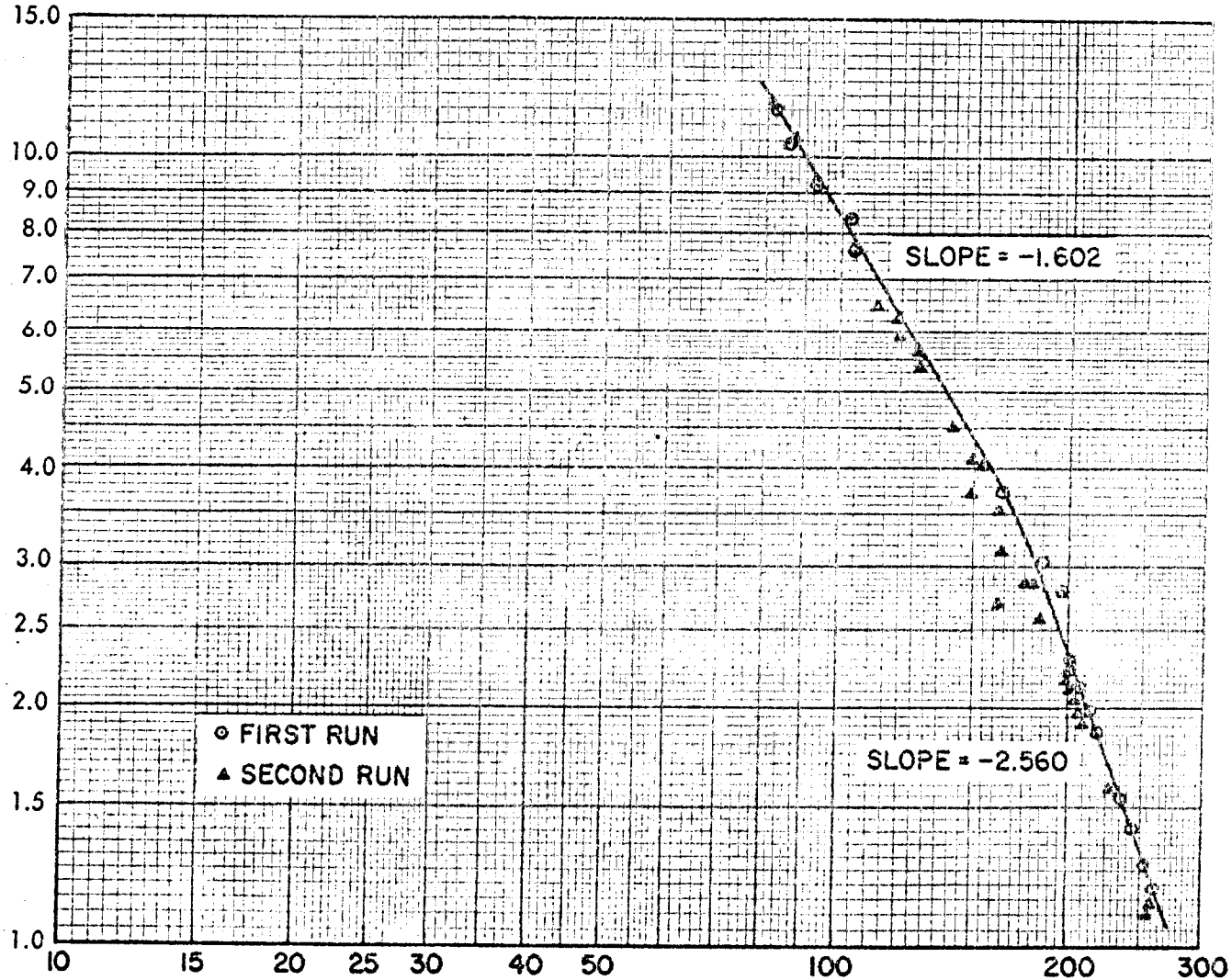

Figure 2-10–Log $\mu \times 10^3$ versus Log T for p-type PbTe.

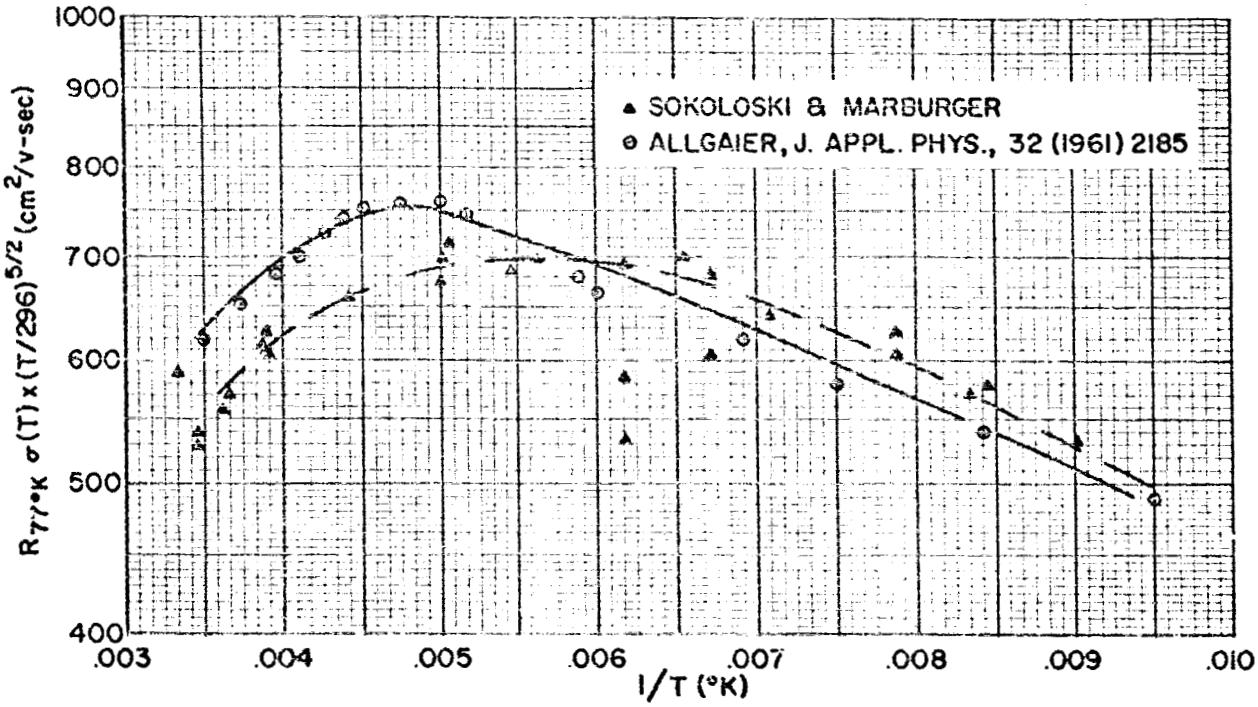

Figure 2-11—Log $R_{77°K}\ \sigma\ (T)\ (T/296)^{5/2}$ Versus 1/T (°K) For p-type PbTe (after Allgaier: J. Appl. Phys. Supp., 32 (1961) 2185

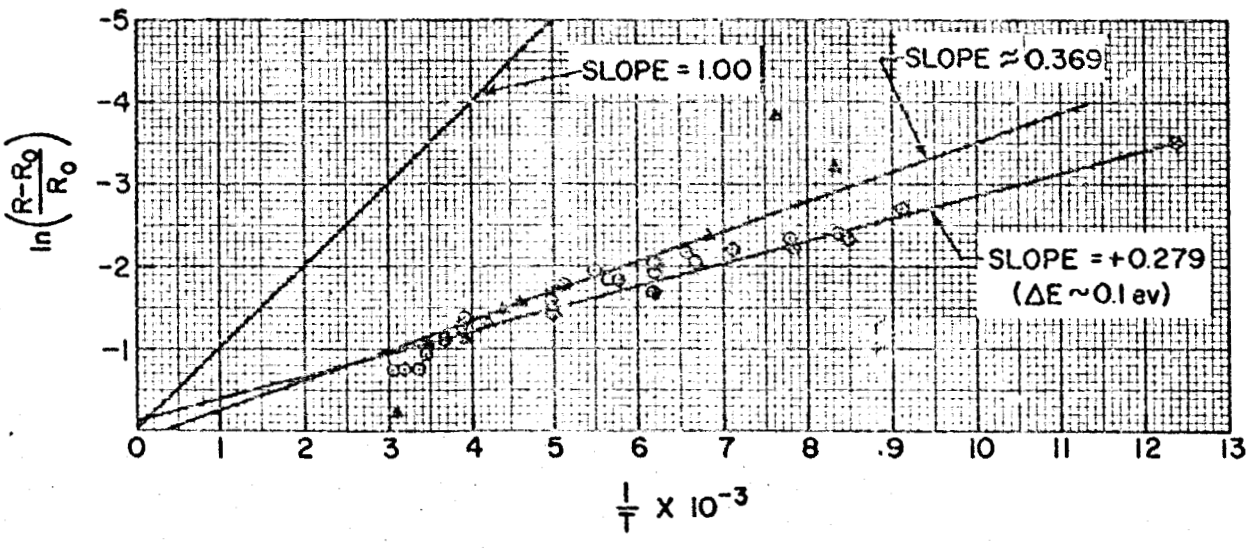

Figure 2-12—A Plot Of Ln $(R-R_o) / R_0$ Versus 1/T.

slope is consistent with that of Allgaier's and supports the conclusion that the difference between these bands is approximately 0.1 ev. However, the following two assumptions made in this calculation are very stringent. The factor, r, which depends on the type of scattering and statistics, changes quite a bit from 1.6 to 2.56, and the Hall coefficient also assumed nearly constant changes by a factor of more than 40%. Therefore, any values obtained from these calculations and assumptions should be looked upon as being a very rough approximation. Lyden (Reference 1) and Miller, et al. (Reference 11) report no significant change in the Hall coefficient in the extrinsic range. Of course conclusions derived from equation (2-3) ignore any temperature dependence of the parameters A and B. However, additional research on p-type PbTe (Reference 12) indicates that the persistence of the temperature dependence of the Hall coefficient in the extrinsic region to such a high carrier concentration makes the explanation of two valence bands less likely. Possible explanation can be attributed to nonparabolic valence bands (Reference 12) and/or to the temperature dependence of the effective masses. Appendix A shows that the two valence band model may be verified by measuring the dependence of the Hall coefficient on the magnetic field strength. This is only true, as pointed out in the appendix, if the single band model Hall coefficient does not depend on the magnetic field strength. Since the Hall coefficient for one carrier does depend on $\omega\tau$ where,

$$\omega = \frac{eH}{m_e}$$

τ = relaxation time of the carriers
(constant for very degenerate temperatures)

a "cut-off" resonance ω_o may be feasible where below this point the assumption $\omega\tau \ll 1$ is valid. Then the conditions reached in Appendix A would be applicable for $\omega < \omega_o$, if τ is constant. This is beyond the scope of this present report, and will be investigated in a future report.

Since only one run was made in the intrinsic range, any conclusions will be pure speculation. Nevertheless, a glance at the conductivity curve in Figure 2-13 shows some consistency with that of Shogenji and Uchiyama in the intrinsic region (Reference 13). The Hall coefficient versus the reciprocal of the temperature curve shows a reversal near 481°K which is consistent with past results of other investigators (References 13 and 14). But the negative branch overshoot has not been reported by anyone. This negative branch overshoot occurs approximately at 542°K. Since some investigators report no irreversible effects until 800°K, the negative branch overshoot phenomena could not

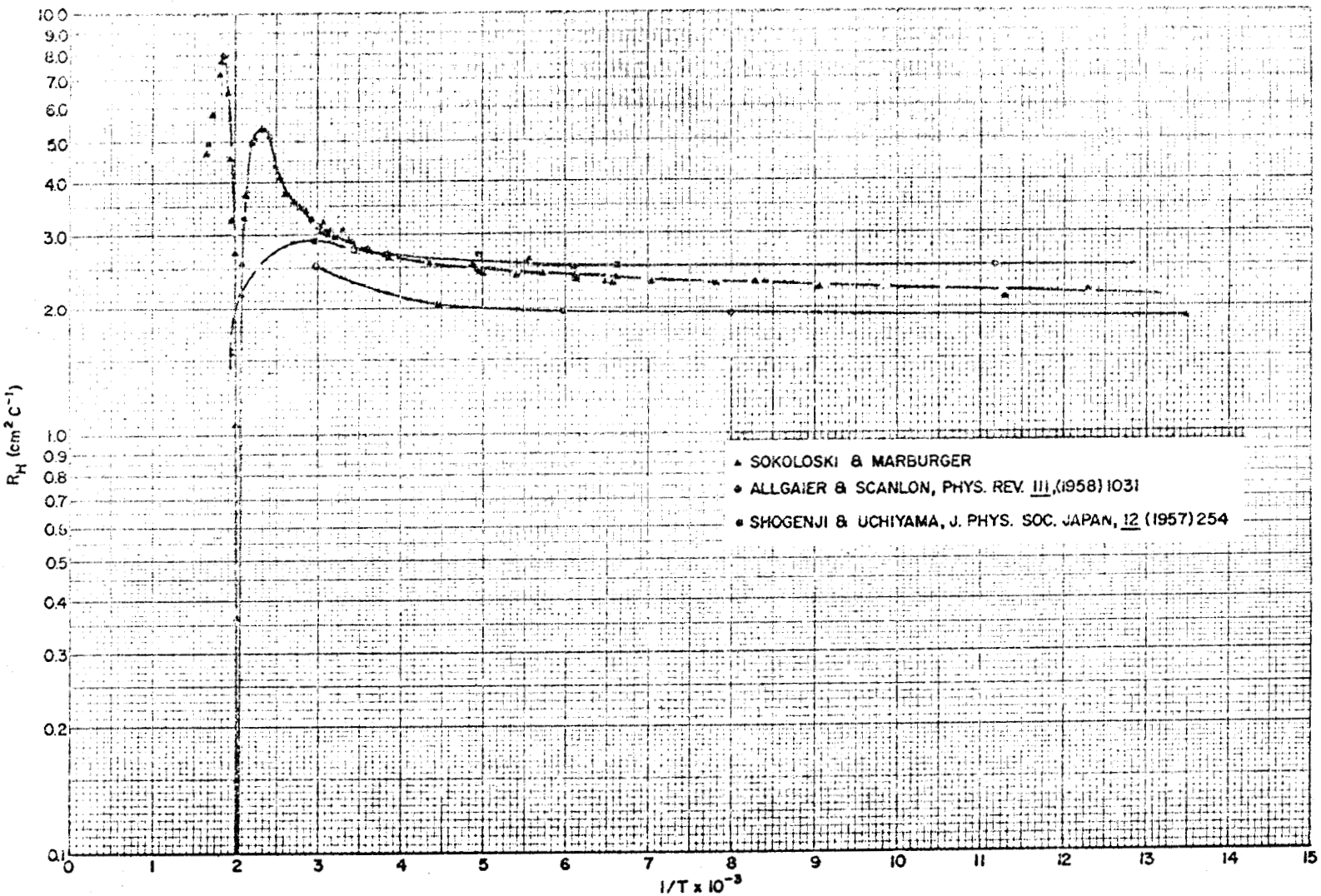

Figure 2-13—Log σ Versus 1/T For p-type PbTe.

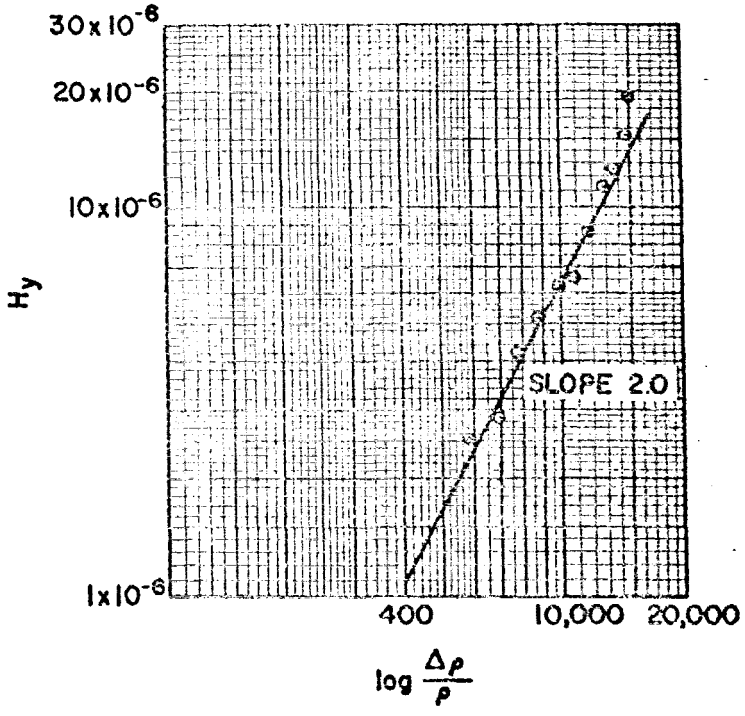

Figure 2-14—Log ($\Delta \rho / \rho$) Versus Log H_y (Room Temp.)

be attributed to this (References 14, 15). Also the sample was encapsulated with Saureisen cement and heated in one atmosphere of argon at all times. Miller et al. state that any reaction that may have occurred between the cement and the specimen did not affect their results significantly. Also a very small percentage change (no value was given) was observed in the room temperature resistance after repeated thermal cycling on an encapsulated sample (Reference 11). Putley (Reference 14) and more recently Uchiyama and Shogenji (Reference 13) report anomolies in p-type PbTe doped with copper, but these results were observed on the Hall coefficient in the extrinsic region. Nevertheless, a negative branch overshoot implies a mobility ratio of greater than 3.7, while those mentioned in the literature range from 1.5 to 2.5 (References 13 and 14). Figure 2-14 illustrates the behavior of the transverse magnetoresistance effect for magnetic field strengths up to 17 kilogauss. The change in resistance is proportional to H_y^2.

Figure 2-15 shows the results of a trial run of the thermoelectric power measurement on Bi_2Te_3 using the Ioffe type apparatus described in the last section. The dashed curve shows the effect of irreversible phenomena similar to that of PbTe above 800°K. Aside from the irreversible effects, the measurements made below the irreversible temperature are consistent and reproducible.

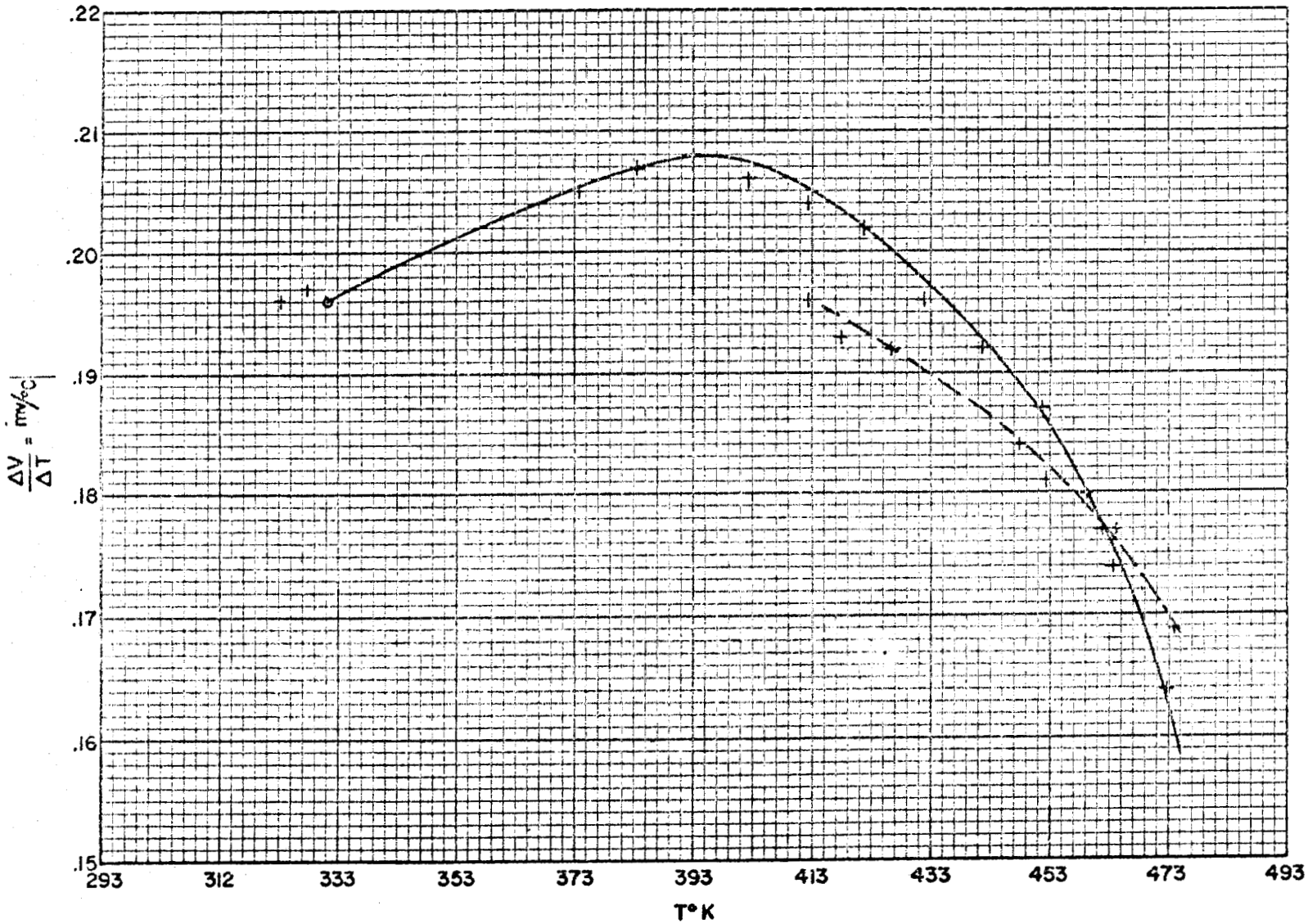

Figure 2-15—Seebeck Voltage Of Bi_2Te_3 Versus T.

SECTION IV

ANALYSIS OF ERROR

The geometry of the sample is shown in Figure 2-16.

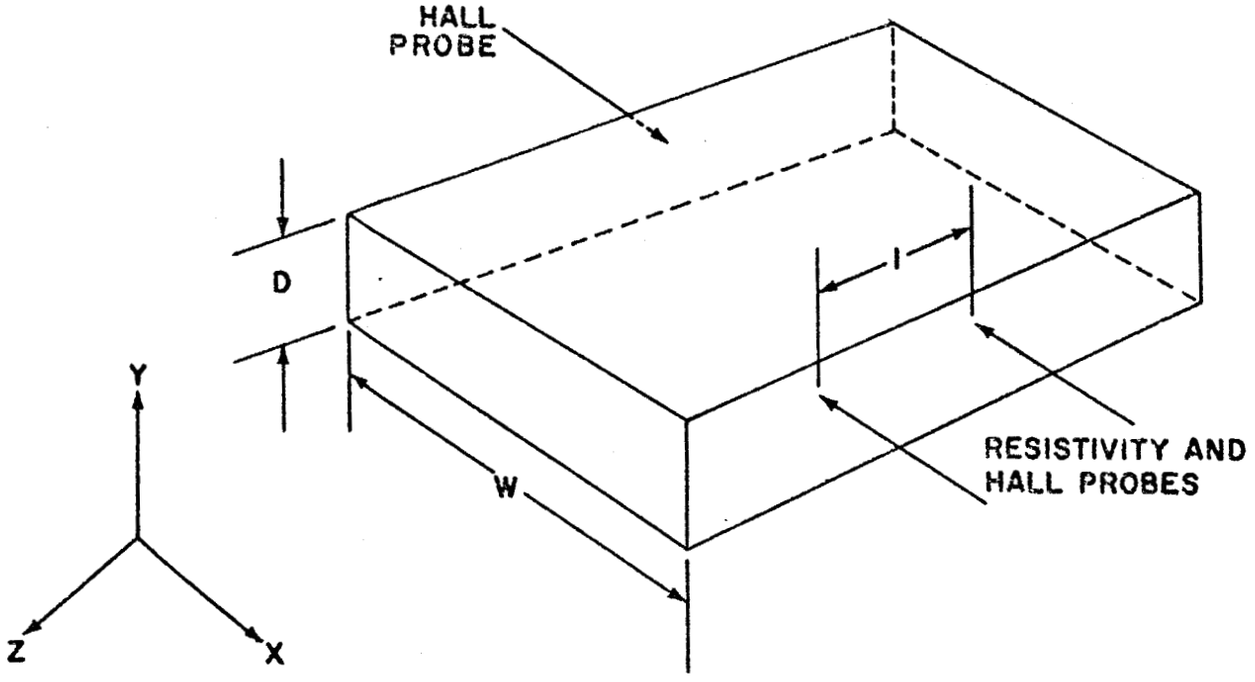

Figure 2-16

A. ELECTRICAL CONDUCTIVITY

The formula for the electrical conductivity is

$$\sigma = \frac{I_z}{V_z} \frac{\ell}{wd}$$

where:

I_z = sample current

V_z = sample voltage

ℓ = distance between resistivity probes

w = width of the sample

d = depth of the sample

From statistical error theory, the total standard deviation in the calculated quantity is given by:

$$S_\sigma = \left[\left(S_{I_z}\frac{\partial\sigma}{\partial I_z}\right)^2 + \left(S_{V_z}\frac{\partial\sigma}{\partial V_z}\right)^2 + \left(S_\ell\frac{\partial\sigma}{\partial\ell}\right)^2 + \left(S_w\frac{\partial\sigma}{\partial w}\right)^2 + \left(S_d\frac{\partial\sigma}{\partial d}\right)^2\right]^{1/2} *$$

where,

$$S_x = \left[\frac{\sum_1\left(\bar{x} - x_g\right)^2}{n-1}\right]^{1/2} \quad ; \quad \begin{array}{l}\bar{x} = \text{mean of population}\\ n = \text{number of occurrences}\end{array}$$

Since the calculation of S_σ for each measurement is more exact but, alas, time consuming, only the value of S_σ for a typical measurement of σ shown in Table 2-1 was calculated. From Table 2-2 the value of S_σ and the percentage standard deviation from the mean, $\frac{S_\sigma}{\bar{\sigma}}$ were 18.48 and .725% respectively. The method for averaging V_z requires some explanation. Since the value of V_z may be complicated by Seebeck and Peltier voltages, the average of two means (the mean of the voltage with I_z in one direction and the mean with I_z in the other) is used. Mathematically a weighting factor should be used in computing the final mean and standard deviation, but this was ignored. Although the variables associated with the sample dimensions (d & w) account for a large percentage of the total error, these can be labeled pseudo-systematic errors for this particular sample. The justification for ignoring these errors is that they are redundant and constant for all experiments associated with this sample. Nevertheless, these errors, due to d and w, must be accounted for when more than one sample with different geometries are being calculated and compared. Therefore, setting $S_d = S_w = 0$

$$S_\sigma \text{ (Sample \#1)} = \left[\left(S_{I_z}\frac{\partial\sigma}{\partial I_z}\right)^2 + \left(S_\ell\frac{\partial\sigma}{\partial\ell}\right)^2 + \left(S_{V_z}\frac{\partial\sigma}{\partial V_z}\right)^2\right]^{1/2} = 2.274$$

*Throughout these calculations, no correlation of errors was assumed.

and:

$$\frac{S_\sigma}{\bar{\sigma}} = 0.08\%$$

As a result the total error for the electrical conductivity should not vary more than 0.08% for one sample; i.e., sample #1.

B. HALL COEFFICIENT

Since S_{H_y} was not exactly known, the procedure here will be to find an upper bound for the error in the Hall coefficient. Table 2-3 shows values for S_{R_H} and $\frac{S_{R_H}}{\bar{R}_H}$ for $S_{H_y} = 0$. Next a calculation is made to find the error in H_y (given values from Table 2-3 for S_d, S_{I_z}, and S_{V_x}) for $S_{R_H} = 0.05$ or a percentage standard deviation from the mean of 5%.

$$S_{H_y} = \left[S_{R_H} - \left(S_d \frac{\partial R_H}{\partial d} \right)^2 - \left(S_{V_x} \frac{\partial R_H}{\partial V_x} \right)^2 - \left(S_{I_z} \frac{\partial R_H}{\partial I_z} \right)^2 \right]^{1/2} \left(\frac{H_y}{R_H} \right)$$

$$\approx \pm 25.69 \text{ Gauss}$$

while:

$$\frac{S_{H_y}}{\bar{H}_y} \approx 0.8\%$$

Since readings of better than $\pm$ 25 Gauss were made, the experimental error of R_H should be less than 5%.

C. HALL AND CONDUCTIVITY MOBILITIES

The formula for the Hall mobility is:

$$\mu_H = \sigma R_H$$

Since the conductivity mobility differs only by a constant factor from the Hall mobility, the errors for both will be the same.

$$S_{\mu_c} = S_{\mu_H} = \left[\left(S_\sigma \frac{\partial \mu_H}{\partial \sigma}\right)^2 + \left(S_{R_H} \frac{\partial \mu_H}{\partial R_H}\right)^2\right]^{1/2}$$

$$= \sqrt{\left(S_\sigma \cdot R_H\right)^2 + \left(S_{R_H} \cdot \sigma\right)^2}$$

$$\approx 0.01190 \times 10^3$$

while:

$$\overline{\mu}_H = \langle \sigma R_H \rangle$$

$$= 5.949 \times 10^3$$

$$\frac{S_{\mu_H}}{\overline{\mu}_H} = 0.2\%$$

D. CARRIER CONCENTRATION

The formula for the carrier concentration is

$$n = \frac{1}{R_H e}$$

for degenerate statistics or high magnetic field strengths.

$$\therefore \quad S_n = S_{R_H} \cdot \frac{1}{R_H^2 e}$$

$$\frac{S_n}{n} = \frac{S_{R_H}}{R_H} = 2\%$$

E. MAGNETORESISTIVITY

The formula for the magnetoresistivity is

$$M_T = \frac{\Delta\rho}{\rho}$$

where:

$$\Delta\rho = \rho(H_y) - \rho(o)$$

or

$$M_T = \frac{\Delta V_z}{V_z}$$

$$\therefore \quad S_{M_T} = S_{V_z}$$

$$\frac{S_{M_T}}{M_T} = \frac{S_{V_z}}{V_z} = 1.2\%$$

Table 4 summarizes all the errors, both estimated and calculated encountered in this report.

TABLE 2-1

I_z (amps)	$\overline{I_z}$	S_{I_z}	$\frac{S_{I_z}}{\overline{I_z}}$
0.090258 0.090250 0.090242 0.090236	0.0902465	9.55×10^{-6}	0.01%
V_x (volts)	$\overline{V_x}$	S_{V_x}	$\frac{S_{V_x}}{\overline{V_x}}$
20.0×10^{-6} 20.9 20.7 20.3	20.47×10^{-6}	0.401×10^{-6}	1.95%
V_z (volts)	$\overline{V_z}$	S_{V_z}	$\frac{S_{V_z}}{\overline{V_z}}$
167.5×10^{-6} 167.3 (1)	167.40×10^{-6}	0.141×10^{-6}	0.08%
177.6 181.7 (2)	179.64×10^{-6}	2.9×10^{-6}	1.6%
Mean (1) & (2)	173.52×10^{-6}	1.52×10^{-6}	1.2%
	$\overline{w}$ 0.31701 cm	S_w 2.006×10^{-3}	
	$\overline{d}$ 0.30892 cm	S_d 1.152×10^{-3}	
	$\overline{l}$ 0.47965 cm	S_l 6.57×10^{-5}	

TABLE 2-2

Source of Error	Error (1)	Partial Derivative (2)	Contribution to Total (1) × (2) = (3)	Square of Contribution
I_z amps	9.55×10^{-6}	$\sigma \cdot \frac{1}{I_z} = 2.8227\times10^{4}$	0.26957	0.07267
V_x volts	0.401×10^{-6}	←		→
V_z volts	1.52×10^{-6}	$\sigma \cdot \frac{1}{V_z} = -1.4680\times10^{7}$	2.23136	4.97897
w cm	2.006×10^{-3}	$\sigma \cdot \frac{1}{w} = -8.03555\times10^{3}$	16.11913	259.8321
d cm	1.152×10^{-3}	$\sigma \cdot \frac{1}{d} = -8.24598\times10^{3}$	9.4994	90.2386
l cm	6.57×10^{-5}	$\sigma \cdot \frac{1}{\ell} = 5.3108\times10^{3}$	0.34891	0.12174
			TOTAL	355.244

The error of σ expressed as the standard deviation, is then

$$S_\sigma = \sqrt{355.244} = 18.48$$

and the fractional error (percent standard deviation from the mean).

$$\frac{S_\sigma}{\bar{\sigma}} = 0.725\%$$

where

$$\bar{\sigma} = \left\langle \frac{I_z\, \ell}{V_z\, wd} \right\rangle$$

$$= 2.547\times 10^{3}$$

TABLE 2-3

Source of Error	Error	Partial Derivative	Contribution to Total	Square of Contribution
H_y Gauss	0.00	$R_H \cdot \frac{1}{H_y} = 0$		
V_x volts	0.401×10^{-6}	$R_H \cdot \frac{1}{V_x} = 1.14 \times 10^{5}$	4.575×10^{-2}	2.093×10^{-3}
I_z amps	9.55×10^{-6}	$R_H \cdot \frac{1}{I_z} = 25.880$	2.472×10^{-4}	6.108×10^{-9}
d cm	1.152×10^{-3}	$R_H \cdot \frac{1}{d} = 7.56053$	8.91×10^{-3}	7.5×10^{-5}
			TOTAL ≈	2.093×10^{-3}

The error of R_h expressed as the standard deviation, is then

$$S_{R_H} = \sqrt{2.093 \times 10^{-3}} = 0.04575$$

and the fractional error (per cent standard deviation from the mean).

$$\frac{S_{R_H}}{\overline{R_H}} = \frac{0.0475}{2.3356}$$

$$= 2\%$$

where

$$\overline{R_H} = 10^8 \left\langle d \frac{V_x}{I_z H_y} \right\rangle \left(\frac{cm^3}{COUL} \right)$$

H_y = Magnetic Field

V_x = Hall Voltage. For other symbols see pages 23 and 24.

TABLE 2-4

SUMMARY OF ERRORS

Quantity	Calculated	Estimated
R_H	2%	2%
$\sigma(d = w = o)$	0.7%	0.28%
n(79°K)	2%	2%
μ_H and μ_c	0.2%	2.2%
M_T	1.2%	1.6%
θ	3%	

SECTION V

CONCLUSION

Undoubtedly more work is needed to determine the mechanism involved in the dependence of the Hall coefficient on temperature in the extrinsic region. Kanai et al have done some high field measurements on n-type PbTe at various temperatures, using pulsed magnetic fields (Reference 16). The dependence of the Hall coefficient at high field strengths should be very interesting just to see if the high field approximations would be approached (see Appendix A). Riedl has done some optical absorption measurements on p-type PbTe at various temperatures. The curve giving the absorption coefficient versus wavelength at 195°K shows three absorption peaks - one is associated with transitions across the gap, the second with intra-band free carrier absorption centers (Reference 17) and the third is unexplained. There is strong correlation between this and the behavior of the Hall coefficient as a function of temperature in the extrinsic range. More calculations and investigations should be made in this area.

Acknowledgments:

We would like to acknowledge the help of Dr. Felix E. Geiger and Mr. Fred G. Cunningham for their encouragement and assistance.

SECTION VI

APPENDIX A

THE DEPENDENCE OF THE HALL COEFFICIENT AT DEGENERATE TEMPERATURES ON INDUCTION FOR CONDUCTION IN TWO VALENCE BANDS

The relationship between the Fermi energy, E_F; density of states effective mass for holes, m_H^*; hole concentration p_i; and temperature is given by,

$$p_i = 4\pi\left(\frac{2 m_H^* kT}{h^2}\right) F_{1/2}\left(\frac{E_F}{kT}\right) \quad \text{(Reference 18)} \tag{A-1}$$

where k and h are Boltzmans and Planks constants respectively. This can be rearranged to yield,

$$F_{1/2}(\eta) = \frac{P_i}{4\pi}\left[\left(\frac{h}{m_e}\right)\frac{h}{m_H^* kT}\right]^{3/2} \tag{A-2}$$

where $\eta = \frac{E_F}{kT}$ is the reduced Fermi energy. The latest value of m_H^* is 0.14 m_e at 77°K (Reference 1) and $p_i = 2.6 \times 10^{18}/cm^3$ at 77°K from the Hall coefficient measured in this experiment. With these respective values (A-2) becomes

$$F_{1/2}(\eta) = 4.32 \tag{A-3}$$

and

$$\eta = 3.2 \quad \text{(Reference 19)}$$

This value signifies that p-type PbTe with a carrier concentration of $2.6 \times 10^{18}/cm^3$ holes is very degenerate at 77°K. As a matter of fact

$$\tau = \ell E^{1/2} \tag{A-4}$$

where τ is the relaxation time, ℓ mean free path and E energy and if a great majority of the carriers have energies near or equal to the Fermi energy, E_F, which is a fairly valid assumption for a semiconductor of this degeneracy, then (A-4) becomes

$$\tau = \ell E_F^{1/2} = \text{const.} \quad \text{(Reference 20)} \tag{A-5}$$

Also

$$r = \frac{\langle \tau^2 \rangle}{\langle (\tau) \rangle^2} = 1 \tag{A-6}$$

so that the Hall coefficient for a degenerate semiconductor, with spherical bands and one carrier, holes, becomes

$$R_H = \frac{r}{n_i e} = \frac{1}{n_i e} \tag{A-7}$$

where n_i is the number of extrinsic carriers

It is well known that the Hall coefficient for infinite inductions is

$$R_{B\to\infty} = \frac{1}{ne}.$$

The Hall coefficient for a simple one carrier, very degenerate semiconductor is independent of field strength, B. (This can be seen to be a limiting case for p = o, and degenerate statistics, $\xi > 3$, in figures VIII 7 and VIII 8 in Reference 20.)

The weak field Hall coefficient for hole-hole conduction in the valence band at degenerate temperatures is

$$R_o = \frac{n_1 c^2 + n_2}{e(n_1 c + n_2)^2} \qquad \text{(A-8)}$$

where n_1 and n_2 are the number of holes in bands one and two respectively, and $c = \frac{\mu_1}{\mu_2}$ is the ratio of mobility in bands one and two. The ratio of the weak field approximation of the Hall coefficient to the strong field Hall coefficient at degenerate temperatures is given by

$$\frac{R_o}{R_\infty} = \frac{f_1 c^2 + f_2}{(f_1 c + f_2)^2} \qquad \text{(A-9)}$$

where $R_\infty = \frac{1}{n_1 + n_2}$, and f_1 and f_2 are the fractional number of carriers in bands one and two respectively, $f_1 + f_2 = 1$. The inequality

$$f_1 (c-1)^2 - f_1^2 (c-1)^2 > 0 \qquad \text{(A-10)}$$

is valid for $f_1 < 1$ and $c \neq 1$, which are extremely liberal conditions.

For p-type PbTe, the Hall coefficient increases from 79°K to the end of the extrinsic range (Reference 7), therefore, the conclusion that

$f_1 < 1$ is well warranted. For the case $c \neq 1$, the conclusion

$$\frac{R_o}{R_o} > 1 \qquad \text{(A-11)}$$

is correct. For a two band valence model obeying degenerate statistics the weak field Hall coefficient is seen to be greater than the strong field Hall coefficient. Is there a region where this is not true?

The Hall coefficient for a degenerate semiconductor is given by

$$R(H^2) = \frac{1}{e} \frac{\frac{\sigma_1^2}{n_1} + \frac{\sigma_2^2}{n_2} + \left(\frac{H}{e}\right)^2 \frac{n_1 - n_2}{n_1^2 n_2^2} \sigma_1^2 \sigma_2^2}{\left(\sigma_1 + \sigma_2\right)^2 + \left(\frac{H}{e}\right)^2 \frac{\left(n_1 - n_2\right)^2}{n_1^2 n_2^2} \sigma_1^2 \sigma_2^2} \quad \text{(Reference 21)} \qquad \text{(A-12)}$$

where σ_1 and σ_2 are the conductivities in bands one and two, respectively. For the assumptions here, spherical energy surfaces and constant τ, there will be no change in σ_1 or σ_2 due to a transverse magnetic field (Reference 22). σ_1 and σ_2 satisfies the following formula

$$\sigma_i = n_i e \mu_i \qquad i = 1 \text{ or } 2 \qquad \text{(A-13)}$$

Substituting (A-13) into (A-12) and simplifying the expression for $R(H^2)$ becomes:

$$R(H^2) = \frac{e\left(n_1 \mu_1^2 + n_2 \mu_2^2\right) + e\left(\mu_1 \mu_2\right) N H^2}{e^2\left(n_1 \mu_1 + n_2 \mu_2\right)^2 + e^2\left(\mu_1 \mu_2\right)^2 N^2 B^2} \qquad \text{(A-14)}$$

where N is the total number of impurities and is constant. After the following terms are defined

$$\alpha = (\mu_1\mu_2)^2 N^2 H^2 \rho^2$$

and

$$\rho = (n_1\mu_1 + n_2\mu_2)^{-1} \tag{A-15}$$

equation (A-14) reduces to

$$R(H^2) = \frac{R_o + \frac{1}{e}\alpha}{1 + N\alpha} \tag{A-16}$$

where R_o is defined in (A-8). Differentiating (A-16) with respect to H^2 (α depends on H^2) will yield the dependence of R on H between R_o R_∞

$$\frac{\partial R(H^2)}{\partial (B^2)} = \frac{(\mu_1\mu_2)^2 N \rho^2}{e} \cdot \frac{\left(1 - \frac{R_o}{R_\infty}\right)}{(1 + N\alpha)^2} \tag{A-17}$$

It is clearly seen, with the help of (A-11), that $R(H^2)$ is a monotonically decreasing function of H^2, since (A-17) is always negative.

SECTION VIII

REFERENCES

(1) Lyden, H. A., MIT Energy Conversion & Semiconductors Lab., Electrical Engin. Dept., Sci. Rept. 7., pg. 86.

(2) Ibid, pg. 97.

(3) Allgaier, R. S., J. Appl. Phys., 32 (1961) 2188.

(4) Long, D., J. Appl. Phys., 33 (1962) 1694.

(5) Cowles, L. E. J., and Dauncey, L. A., J. Sci. Inst., 39 (1962) 16.

(6) Sokoloski, M. M., and Geiger, F. E., NASA Tech. Note D-1695.

(7) Ioffe, A. F., Semiconductor Thermoelements and Thermoelectric Cooling, Infosearch Ltd., London, 1957, pg. 132.

(8) Marburger, J. H. III, NASA Tech. Note D-1840.

(9) Allgaier, R. S., and Scanlon, W. W., Phys. Rev., 111 (1958) 1037.

(10) Op. Cit., Allgaier, R. S., pg. 2187.

(11) Miller, E., Komarek, K., and Cadoff, I., J. Appl. Phys., 32 (1961) 2459.

(12) NOL, Appl. Phys. Dept., NOLTR 62-125 (1962) 6.

(13) Shogenji, K., and Uchiyama, S., J. Phys. Soc. Japan, 12 (1957) 254.

(14) Putley, E. H., Proc. Phys. Soc. B, 68 (1954) 22.

(15) Smith, R. A., Physica, 20 (1954) 920.

REFERENCES (Continued)

(16) Kanai, Y., Nii, R., and Waanabe, n., J. Appl. Phys., 32 (1961) 2146.

(17) Riedl, H. R., Phys. Rev., 127 (1962) 163.

(18) Smith, R. A., Semiconductors (Cambridge University Press, Cambridge, 1959) pg. 79, Equation (20).

(19) McDougall, J., and Stoner, E. C., Phil. Trans. Roy. Soc. 237 (1938) 67.

(20) Op. cit., Smith, R. A., pg. 118.

(21) Wilson, A. H., The Theory of Metals (Cambridge University Press, London, 1958) pg. 237-239.

(22) Ibid., pg. 213, Equation (8.521.9).

(23) Op. cit., Smith, R. A., pg. 105.